

Review

Riding the Plane Wave: Considerations for In Vivo Study Designs Employing High Frame Rate Ultrasound

Jason S. Au ^{1,2} , Richard L. Hughson ^{2,3} and Alfred C. H. Yu ^{1,2,*}

¹ Department of Electrical and Computer Engineering, University of Waterloo, Waterloo, ON N2L 3G1, Canada; jason.au@uwaterloo.ca

² Schlegel-University of Waterloo Research Institute for Aging, Waterloo, ON N2J 0E2, Canada; hughson@uwaterloo.ca

³ Department of Kinesiology, University of Waterloo, Waterloo, ON N2L 3G1, Canada

* Correspondence: alfred.yu@uwaterloo.ca; Tel.: +1-519-888-4567 (ext. 36908)

Received: 15 January 2018; Accepted: 13 February 2018; Published: 14 February 2018

Abstract: Advancements in diagnostic ultrasound have allowed for a rapid expansion of the quantity and quality of non-invasive information that clinical researchers can acquire from cardiovascular physiology. The recent emergence of high frame rate ultrasound (HiFRUS) is the next step in the quantification of complex blood flow behavior, offering angle-independent, high temporal resolution data in normal physiology and clinical cases. While there are various HiFRUS methods that have been tested and validated in simulations and in complex flow phantoms, there is a need to expand the field into more rigorous in vivo testing for clinical relevance. In this tutorial, we briefly outline the major advances in HiFRUS, and discuss practical considerations of participant preparation, experimental design, and human measurement, while also providing an example of how these frameworks can be immediately applied to in vivo research questions. The considerations put forward in this paper aim to set a realistic framework for research labs which use HiFRUS to commence the collection of human data for basic science, as well as for preliminary clinical research questions.

Keywords: high frame rate ultrasound; ultrafast ultrasound; human studies; neurovascular control

1. Introduction

Advancements in diagnostic ultrasound have allowed for a rapid expansion of the quantity and quality of non-invasive information that clinical researchers can acquire from cardiovascular physiology. As a primary application, quantification of blood flow through Doppler ultrasound is useful for the identification of early disease states or diagnosis of pathological conditions either as consequence, or root cause, of altered hemodynamics [1,2]. These applications range across multiple organ systems, for instance, grading conduit artery stenoses by flow jet velocity [3,4], estimating mitral valve inflow for left ventricular diastolic dysfunction [5], or identifying locations at risk for atherosclerotic plaque development by low/oscillatory wall shear stress [6]. However, much of the current technology is limited by assumptions of laminar flow and slow-moving blood flow in a small acoustic window, which restrict most applications to imaging with fixed insonation angles and simple flow patterns.

In recent years, high frame rate ultrasound (HiFRUS; also termed ‘ultrafast’ ultrasound) imaging techniques have been developed to address the above limitations by insonating a large area with unfocused beams through either spherical or plane wave emissions [7]. Rather than being limited by line-by-line pulse-echo imaging, HiFRUS techniques acquire full-field data at very high frame rates (e.g., 1000–10,000 frames per second) for excellent temporal resolution, and allow

beamforming in any direction for angle-independent blood velocity estimations. These advancements enable accurate quantification of high-velocity non-laminar flows, demonstrated both in vivo and in geometrically-realistic phantoms at vessel bifurcations [8–10], aneurysms [11], and even 3D structures such as the left ventricle [12,13]. However, the ability for basic science or clinical researchers to access the vast amount of biological information has so far been limited, with recent HiFRUS reviews touting only the perceived potential of these advances in imaging [7,14–16].

The major challenges for mainstream adoption of HiFRUS technology stem from the lack of large sample human data, as well as descriptive studies of normal and pathological physiology. In this review, we provide a practical framework for basic science researchers conducting preliminary in vivo studies with the long-term objective of clinical relevance. Here, we propose a guideline for standards in technical reporting, and provide considerations for investigations in humans, data management, and storage, as well as a narrative example of how studies could be designed for in vivo observations in basic science questions. Although this review focuses on relevant cardiovascular applications, we encourage the readers to extend these principles to other areas of research which may benefit from HiFRUS imaging.

2. A Synopsis of High Frame Rate Ultrasound Technology

Before we proceed to discuss how in vivo investigation protocols for HiFRUS can be designed, let us first briefly review the current state-of-the-art in HiFRUS technology. While the notion of HiFRUS imaging with sub-millisecond time resolution has been in conception since the 1980s [17], the technology has garnered significant attention since the turn of this decade [18]. Such a rapid surge of interest is technically attributed to two engineering innovation trends. First, in the past decade, reconfigurable ultrasound scanners have become more prevalent [19–24], as opposed to non-programmable clinical systems that are designed via an embedded system approach [25]. These open-architecture systems have enabled researchers to readily implement different variants of unfocused pulsing sequences that are essential for realizing HiFRUS [26]. Second, high-throughput computing hardware such as graphical processing units have greatly matured [27]. These parallel processing devices have served well to achieve real-time execution of HiFRUS-related computation tasks, such as pixel-by-pixel beamforming [28–30], Doppler processing [31–33], and post hoc filtering [34].

At present, a number of academic labs have developed in-house research scanners with HiFRUS capabilities. Worth particular mention are the in-house systems built at the Technical University of Denmark [19,23], the University of Florence [21,24], the Langevin Institute in Paris [35], and the Polish Academy of Sciences [36]. A few commercially available research platforms also allow similar HiFRUS implementations, such as Analogic Ultrasound (Peabody, MA, USA) [37], Verasonics (Kirkland, WA, USA) [22], US4US (Warsaw, Poland), and Cephasonics (Santa Clara, CA, USA). Note that most conventional ultrasound scanners cannot be readily reconfigured to implement HiFRUS because their architecture is typically developed through an embedded system design approach that only specializes in performing beamline-based imaging [25]; this is why research scanners have become essential for advances in diagnostic ultrasound. Another point worth noting is that one clinical scanner developer (Supersonic Imagine, Aux-du-Provence, France) is currently dedicated to the development of the HiFRUS market [38]. Also, specialized HiFRUS flow vector imaging modes are available on clinical scanners developed by Analogic Ultrasound (Peabody, MA, USA) [39] and Mindray (Shenzhen, China) [40].

In terms of its technical principles, HiFRUS imaging is fundamentally instituted upon the pulse-echo sensing paradigm, similar to conventional ultrasound imaging. However, instead of using focused beams for transmission, HiFRUS instead uses unfocused pulsing strategies in the forms of spherical waves [41] or plane waves [18,38], as shown in Figure 1. On reception, the pulse echoes returned from the imaging plane of interest are recorded on every array transducer channel. Pixel-by-pixel beamforming is then performed using the channel-domain pulse-echo data, in which each image pixel value is derived through a “delay and sum” approach [28]. One salient point to

be noted is that the lateral spatial resolution of HiFRUS is inherently not as fine as conventional ultrasound because unfocused transmit firings are used. Nonetheless, the temporal resolution is significantly improved because, from each transmit event's channel-domain data set, it is possible to form one image frame based on pulse-echoes returned from the entire imaging view. To improve the lateral resolution of HiFRUS images, one strategy that can be leveraged is to perform coherent compounding of low-resolution image frames derived from different spherical firing positions [41] or different plane wave steering angles [42]. While this compounding operation would unavoidably reduce the frame rate, it may be carried out recursively to limit the loss in frame rate [43].

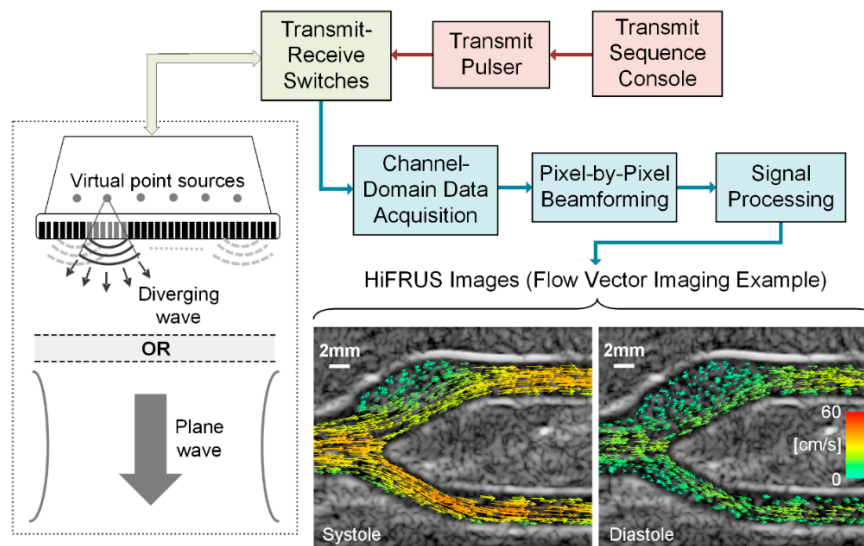


Figure 1. Overview of high frame rate ultrasound (HiFRUS) data acquisition principles and the signal processing chain. Two sample HiFRUS images in the form of flow vector imaging with dynamic visualization [8] are shown in the context of a carotid bifurcation model.

From an application standpoint, the key diagnostic value offered by HiFRUS is the full-field, high-resolution spatiotemporal imaging that can yield functional insight into physiological events taking place inside the human body. For instance, by integrating HiFRUS with Doppler estimation principles, it is possible to achieve time-resolved visualization of complex flow dynamics through the rendering of flow speckles [9] and the derivation of flow vectors at different pixel positions [44] as illustrated in the sample images in Figure 1. Not only is this useful in examining carotid hemodynamics [8,40], it is also applicable to the evaluation of arterial strain [45–47], the visualization of pulse wave propagation through the artery wall [48], and the tracking of shear waves propagating in tissues [35,49]. HiFRUS may also be used in urology applications to gain time-resolved insight into turbulent urinary flow behavior [50]. This technology may be used in cardiac applications to study myocardial contraction [51,52] and intraventricular flow patterns [53,54], although these techniques need further refinement. Emerging developments in HiFRUS methodologies, including the incorporation of contrast agents [55] and state-of-the-art 4D imaging [56], will undoubtedly lead to further physiological discoveries to enhance application prospects in this field.

3. Framework for In Vivo Cardiovascular Studies

The refinement of HiFRUS and blood flow vector quantification has led to a large number of technical descriptions and validation studies, but very few in vivo clinical studies in which the potential for advanced imaging methods can be highlighted. In these limited human studies, the focus has been on proof-of-concept study designs, with small sample sizes, limited a priori hypotheses, and case studies, rather than group comparisons or interventional designs [10,12,13,39,57–59]. Focused studies on basic science or clinical research questions are the natural next step for the field, in which

HiFRUS can be used as a specialized research tool for both simple and complex system cardiovascular measurement. However, in order to build in a level of consistency between the varied methods, HiFRUS research groups should be aware of the technical, physiological, and ethical considerations required for larger scale human studies. Below, we outline such considerations, of which we encourage for high-quality reporting and study design.

3.1. Validation of Methods Prior to In Vivo Data Collection

The range in both hardware and software solutions for HiFRUS platforms introduces a degree of uncertainty in the accuracy and validity of methods during the early stages of system development. As measurement error is an important component of interventional in vivo studies, the accuracy in flow imaging should be determined through validation studies, using either criterion standard methodology (e.g., magnetic resonance imaging [60]), or validated models with known hemodynamic properties (e.g., computational fluid dynamics simulations [61] and flow phantoms [62]). The specific decisions for constructing and validating flow phantoms have been previously reviewed [63], and should be considered prior to diverting resources to human studies.

3.2. Standards in Technical Reporting

While few clinical ultrasound systems have the capability for HiFRUS imaging, certain research systems allow for customization of the transmit firing sequence of every array channel and the acquisition of channel-domain data for customized algorithmic processing [19–24,35–37]. In general, HiFRUS imaging studies rigorously report the technical specifics of the experimental methods, such as the array pitch, probe frequency, transmit pulse duration, pulse repetition frequency, steering angles, and spherical source positioning. As HiFRUS technology is adopted into basic science and clinical research, such details should be preserved and summarized in study reports for easy comparison between methods. Table 1 lists the essential technical reporting that should be ideally described in such studies. In addition to the technical reporting, scanning locations should be rigorously reported, including the organ of interest, relevant landmarks for reproducibility, details on insonation angles (e.g., anterior or lateral plane on the neck), and target organ orientations (e.g., visualization of both the internal and external carotid arteries in the same plane).

Table 1. Technical reporting in high frame rate ultrasound (HiFRUS) investigations and proposed details for the research example presented in Section 4.

HiFRUS Parameter	Value
Scanning system	SonixTouch
Array pitch	0.3048 mm
Probe frequency	5 MHz
Emission method	Plane wave excitation
Transmit pulse duration	2 cycles
Pulse repetition frequency	10 kHz
Steering angles	−10°, 0°, +10°
Slow-time window size (or ensemble length)	128 samples (12.8 ms)
Slow-time window step size	4 samples (0.4 ms)
Effective frame rate	833 fps
Scanning location	Left of image aligned 1 cm proximal to the carotid bifurcation
Collection duration	3 s (16 GB on-board memory)

The majority of clinical ultrasound studies are performed by highly trained sonographers, often hired by clinical research teams. Although research sonographers are highly trained, considerations should be given to any motion artefact caused by human error that may influence data quality during HiFRUS acquisitions. Considering the limited data that can be acquired during study sessions (potentially within a few heart cycles due to data storage and processing as discussed below), it is important to eliminate sources of variability beyond that of the biological system being investigated.

For this reason, probe holders should be considered as part of the experimental set-up when possible, and reported in the study methodology. Stereotactic probe holders have previously been shown to reduce the typical error of the flow-mediated dilation technique, which is based on diameter changes in the brachial artery after a brief period of distal limb ischemia [64].

3.3. Human Considerations

A shift in focus from flow phantoms to human participants brings about certain considerations for in vivo testing that may introduce unwanted variability into data quality. The human cardiovascular system is tightly regulated by the autonomic nervous system, involving beat-to-beat neurovascular regulation through the sympathetic and parasympathetic nervous systems [65,66]. However, this regulation may offer unwanted sources of variability during HiFRUS studies, as only a few cardiac cycles can realistically be acquired per participant due to the high frame rate. Decisions on participant pre-visit instructions and study methodology should be made with consideration on how to minimize these confounders. For example, technical guidelines for evaluations of carotid–femoral pulse wave velocity and flow-mediated dilation have recommended that: participants refrain from food (~2–6 h), caffeine, smoking, and alcohol (~12 h) prior to measurement; testing should occur in a quiet, temperature-controlled room after 10 min of supine rest; and measurements be taken at the same time of day for longitudinal studies to account for circadian rhythm [67–74]. While Table 2 lists recommendations for the average participant, any perturbations from the ‘ambulatory’ state of an individual should be considered; for example, asking an individual who habitually smokes to refrain from smoking may cause an equal amount of distress and undue sympathetic activation. As the novelty of HiFRUS data limits the available literature on the confounders of measurement variability, we suggest that the above basic study controls be considered for studies involving human participants, with the aim of reducing unwanted variability in the high-quality data.

Table 2. Methodological considerations in cardiovascular human testing.

Recommendation	Reason
Pre-visit instructions	
2 h fasted	Altered sympathetic activation
6 h refrain from caffeine	Altered sympathetic activation
12 h refrain from smoking	Acute effects on vascular structure and function
12 h refrain from moderate-to-vigorous physical activity	Acute effects on vascular structure and function
12 h refrain from alcohol	Acute effects on vascular structure and function
Record of current medications	Various acute and chronic effects on the vasculature
Participant preparation	
Assign unlinked participant ID	Ethical considerations for sensitive health information
10 min rest period	Altered sympathetic activation upon arrival to the lab
Resting heart rate recording	Detail of the hemodynamic environment
Resting blood pressure recording	Detail of the hemodynamic environment
Probe holder placement	Reduction of motion artifacts
Breath hold during acquisition	Reduction of motion artifacts

Medications are an important consideration when preparing to interpret the potentially clinically relevant information provided in HiFRUS examinations. As it is unethical and unsafe to ask participants to withhold all medication for certain studies, it is important to record and consider possible confounders when interpreting findings. Particular care should be taken with commonly prescribed medications for hypertension and heart disease, such as statins, beta-blockers, angiotensin-converting enzyme inhibitors, and diuretics, all of which result in measurable effects on cardiovascular function including reductions in heart rate, blood volume and arterial stiffness [67].

Further to the issue of beat-to-beat variability, additional considerations should be given to factors that may affect the ability of individual heart cycles to reflect ‘steady state’ conditions of an individual or physiological state. Respiratory sinus arrhythmia is a known phenomenon in physiological monitoring, eliciting predictable fluctuations in heart rate and blood pressure [75]. Given that typical respiratory

and heart rates in healthy adults are ~20 breaths/min and ~70 beats/min, respectively, an average of at least six heart cycles is necessary to accurately reflect steady state physiology, which may not be feasible for all HiFRUS acquisition systems. Borrowing from echocardiography guidelines, an alternative solution to averaging is implementing brief breath holds to limit both the sympathetic and mechanical effects of breathing [76,77]. Other arrhythmias such as ectopic beats, premature atrial/ventricular contractions, or flutters may cause difficulty in recording steady state data, although arrhythmia physiology may be an interesting study area in itself for HiFRUS examination.

Variable acoustic windows and poor image quality are potential barriers for high quality HiFRUS investigations, which may limit the available participant pool in human studies. While flow phantoms offer complete control of model orientation, depth, and acoustic medium, human studies will certainly produce sub-optimal data quality, which will vary between methods. An additional concern for data quality is the potential waste of time and resources that would accompany data dropout, especially for repeated-measures study designs. To address this concern, we recommend including image quality as an exclusion criterion in ethics applications, whereby individuals are first consented under the local ethics board and are then screened for image quality before the start of the study protocol. If participants are being remunerated for their time, they would have to be provided a pro-rated amount as they have been officially enrolled in the protocol upon giving consent. Regardless of the participant flow, reporting quality metrics, such as the number of unusable images or number and reason for data loss, will provide valuable transparency on HiFRUS methodology. Although designed for randomized control trial use, the CONSORT guidelines provide excellent descriptions of high quality participant reporting, which includes number of participants excluded, participants lost to follow up in repeated measures designs, and participants excluded from analysis [78].

4. Research Example: Neurovascular Control and Complex Blood Flow

The above general recommendations for *in vivo* investigations provide a general framework under which the acquisition and management of human data should be optimally performed in cardiovascular research. In order to supplement these considerations, below we present an example of a simple and realistic study design for a basic science research question, describing each step in the design process from research question to data acquisition.

The most attractive element of HiFRUS for a cardiovascular physiologist is the unprecedented quantity and quality of information that can non-invasively be assessed from the conduit arteries. High temporal and spatial sensitivity of complex blood flow patterns may offer a unique view of traditional cardiovascular techniques that have otherwise been well established in the field. For example, the cold pressor test (CPT) is a well-documented assessment of neurovascular reactivity [79,80], which has a history of central and peripheral responder sub-types [81], and documented effects on intra- and extra-cranial blood flow [82,83]. The CPT is highlighted by its simple protocol: submersion of either the hand or foot into an ice bath (~2–4 °C) for a duration of ~2 min. This stimulus elicits a rapid neurovascular response, characterized by α -adrenergic peripheral vasoconstriction causing slight increases in heart rate (i.e., +5 to +10 beats per minute) and moderate increases in mean arterial pressure (i.e., +15 to +25 mmHg). While recent studies have reported increases in common carotid, internal carotid, and middle cerebral artery blood velocity with the CPT [82,83], it may be of value to characterize the complex flow patterns at the carotid bifurcation to further detail the known hemodynamics of the CPT, as well as to perhaps develop an easily accessible reactivity test for carotid bifurcation jets and recirculation zones under challenge conditions. From this knowledge gap in a well-established cardiovascular technique, we can design an acute interventional within-subject human research question that directly uses the novel capabilities of HiFRUS with *a priori* hypotheses: does the CPT elicit changes in carotid bifurcation flow jet velocity or recirculation zones as measured by HiFRUS?

Figure 2 and Table 1 detail the methodological and technical design elements that we would employ for such a study. Young healthy adults are the ideal participants for this design, as we would like to test a basic science question in a controlled system, ideally by manipulating only the variables

of interest without considering confounding pathology. After institutional safety and ethics approval, participants would be recruited and consented for testing in the lab. To ensure quality data, we suggest that potential participants be screened for appropriate scanning windows for appropriate orientation of the carotid bifurcation (i.e., at minimum, in-plane visualization of the carotid bulb and internal carotid artery). This exclusion criteria limits the generalizability of the experimental findings, but we must acknowledge the variability in carotid geometry in the general population using 2D ultrasound [84,85]. To limit confounding factors for measurement variability, we would ask participants to arrive at the lab having fasted for two hours, and having refrained from moderate-to-vigorous physical activity, smoking, and alcohol in the 12 h prior to assessments (Table 2).

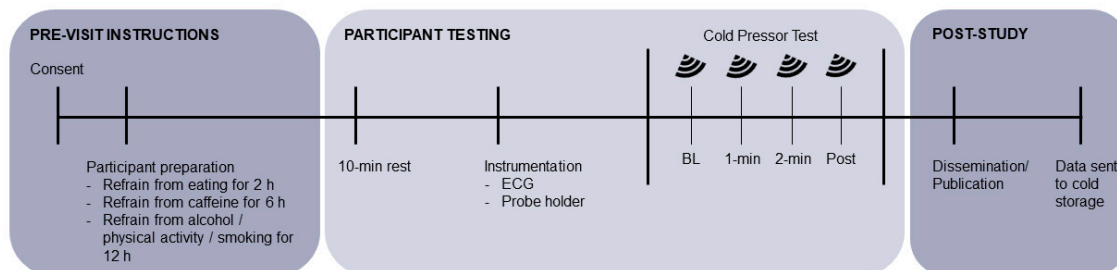


Figure 2. An example of a study timeline and protocol for the experiment outlined in the Research Example. ECG: electrocardiogram.

During the testing protocol, participants would rest supine for at least ten minutes prior to data collection to standardize the hemodynamic environment (i.e., heart rate and blood pressure). For this particular research question, it would be valuable to gate analysis to the electrocardiogram (ECG) trace, in order to account for some beat-to-beat variability in blood flow, as well as to assist with aligning secondary data acquisition such as beat-to-beat blood pressure finger plethysmography or transcranial Doppler signals. A simple single-lead ECG can be used to align the data either on the ultrasound unit, or through simultaneous capture with an external data acquisition system. If possible, participants would be instrumented with a stereotactic probe holder to standardize the anterior–posterior orientation of the ultrasound probe to assist with repeated assessments in the same plane. During acquisition itself, participants would be asked to briefly hold their breath while six heart cycles (~6–8 s; ~16 GB on our system) are recorded. The specific details of the HiFRUS acquisition and analysis would vary between research groups, although we recommend the technical reporting suggested in Table 1 for a fully detailed methods sections to be included for publication.

The above research example is just one of many avenues that HiFRUS methodology may take in cardiovascular science (for other clinical examples, see [7,14–16]). Diagnostic testing in clinical studies presents a unique set of challenges (e.g., power calculations for novel outcomes [86], specificity and sensitivity to detect abnormal hemodynamics [87]), the discussion of which is beyond the scope of this review. Although individual research questions, experimental protocols, and outcome measures may vary, we hope this general description of a research outline may prove useful to researchers beginning to explore the potential for HiFRUS investigations in human participants.

5. Summary

HiFRUS techniques for complex blood flow quantification are being rapidly developed, but have yet to be implemented in larger scale human studies investigating either basic science or clinical research questions. In this paper, we have put forward methodological and technical reporting aspects that should be considered as part of future study designs in the area. Participant preparation, variability controls in experimental protocols, and ethical considerations are just a few of the points that will elevate the research standards in HiFRUS investigations, which we highlight in a practical example in neurovascular control of blood flow. As these techniques are eventually adopted into

larger scale studies, we encourage ultrasound researchers to reach out to partner with physiologists and clinical researchers and extend the possibilities for HiFRUS as an invaluable research tool in cardiovascular science.

Acknowledgments: J.S.A. is funded by a Canadian Institutes of Health Research (CIHR) Post-doctoral Fellowship (MFE-152454). Research funding from the CIHR Project Grant (PJT-153240), Natural Sciences and Engineering Research Council of Canada (RGPIN-2016-04042), Canada Foundation for Innovation (36138), and the Ontario Early Researcher Award (ER16-12-186) is also gratefully acknowledged.

Author Contributions: J.S.A. and A.C.H.Y. contributed to the drafting of this manuscript. J.S.A., R.L.H. and A.C.H.Y. edited and approved the final version of the manuscript.

Conflicts of Interest: The authors declare no conflict of interest.

References

1. Quiñones, M.A.; Otto, C.M.; Stoddard, M.; Waggoner, A.; Zoghbi, W.A. Recommendations for quantification of Doppler echocardiography: A report from the Doppler quantification task force of the nomenclature and standards committee of the American Society of Echocardiography. *J. Am. Soc. Echocardiogr.* **2002**, *15*, 167–184. [[CrossRef](#)] [[PubMed](#)]
2. Rooke, T.W.; Hirsch, A.T.; Misra, S.; Sidawy, A.N.; Beckman, J.A.; Findeiss, L.K.; Golzarian, J.; Gornik, H.L.; Halperin, J.L.; Jaff, M.R.; et al. 2011 ACCF/AHA focused update of the guideline for the management of patients with peripheral artery disease (Updating the 2005 guideline). *Catheter. Cardiovasc. Interv.* **2012**, *79*, 501–531. [[CrossRef](#)] [[PubMed](#)]
3. Steel, R.; Ramnarine, K.V.; Davidson, F.; Fish, P.J.; Hoskins, P.R. Angle-independent estimation of maximum velocity through stenoses using vector Doppler ultrasound. *Ultrasound Med. Biol.* **2003**, *29*, 575–584. [[CrossRef](#)]
4. Oates, C.P.; Naylor, A.R.; Hartshorne, T.; Charles, S.M.; Fail, T.; Humphries, K.; Aslam, M.; Khodabakhsh, P. Joint recommendations for reporting carotid ultrasound investigations in the United Kingdom. *Eur. J. Vasc. Endovasc. Surg.* **2009**, *37*, 251–261. [[CrossRef](#)] [[PubMed](#)]
5. Nagueh, S.F.; Smiseth, O.A.; Appleton, C.P.; Byrd, B.F.; Dokainish, H.; Edvardsen, T.; Flachskampf, F.A.; Gillebert, T.C.; Klein, A.L.; Lancellotti, P.; et al. Recommendations for the evaluation of left ventricular diastolic function by echocardiography: An update from the American Society of Echocardiography and the European Association of Cardiovascular Imaging. *Eur. Heart J. Cardiovasc. Imaging* **2016**, *17*, 1321–1360. [[CrossRef](#)] [[PubMed](#)]
6. Cheng, C.; Tempel, D.; Van Haperen, R.; Van Der Baan, A.; Grosveld, F.; Daemen, M.J.A.P.; Krams, R.; De Crom, R. Atherosclerotic lesion size and vulnerability are determined by patterns of fluid shear stress. *Circulation* **2006**, *113*, 2744–2753. [[CrossRef](#)] [[PubMed](#)]
7. Jensen, J.A.; Nikolov, S.; Yu, A.C.H.; Garcia, D. Ultrasound vector flow imaging—Part II: Parallel systems. *IEEE Trans. Ultrason. Ferroelectr. Freq. Control* **2016**, *63*, 1722–1732. [[CrossRef](#)] [[PubMed](#)]
8. Yiu, B.Y.S.; Lai, S.S.M.; Yu, A.C.H. Vector projectile imaging: Time-resolved dynamic visualization of complex flow patterns. *Ultrasound Med. Biol.* **2014**, *40*, 2295–2309. [[CrossRef](#)] [[PubMed](#)]
9. Yiu, B.Y.S.; Yu, A.C.H. High-frame-rate ultrasound color-encoded speckle imaging of complex flow dynamics. *Ultrasound Med. Biol.* **2013**, *39*, 1015–1025. [[CrossRef](#)] [[PubMed](#)]
10. Hansen, P.M.; Pedersen, M.M.; Hansen, K.L.; Nielsen, M.B.; Jensen, J.A. Demonstration of a vector velocity technique. *Ultraschall Med.* **2011**, *32*, 213–215. [[CrossRef](#)] [[PubMed](#)]
11. Ho, C.K.; Chee, A.J.Y.; Yiu, B.Y.S.; Tsang, A.C.O.; Chow, K.W.; Yu, A.C.H. Wall-less flow phantoms with tortuous vascular geometries: Design principles and a patient-specific model fabrication example. *IEEE Trans. Ultrason. Ferroelectr. Freq. Control* **2017**, *64*, 25–38. [[CrossRef](#)] [[PubMed](#)]
12. Garcia, D.; del Alamo, J.C.; Tanne, D.; Yotti, R.; Cortina, C.; Bertrand, E.; Antoranz, J.C.; Perez-David, E.; Rieu, R.; Fernandez-Aviles, F.; et al. Two-dimensional intraventricular flow mapping by digital processing conventional color-doppler echocardiography images. *IEEE Trans. Med. Imaging* **2010**, *29*, 1701–1713. [[CrossRef](#)] [[PubMed](#)]
13. Hendabadi, S.; Bermejo, J.; Benito, Y.; Yotti, R.; Fernández-Avilés, F.; Del Álamo, J.C.; Shadden, S.C. Topology of blood transport in the human left ventricle by novel processing of doppler echocardiography. *Ann. Biomed. Eng.* **2013**, *41*, 2603–2616. [[CrossRef](#)] [[PubMed](#)]

14. Jensen, J.A.; Nikolov, S.I.; Yu, A.C.H.; Garcia, D. Ultrasound vector flow imaging—Part I: Sequential systems. *IEEE Trans. Ultrason. Ferroelectr. Freq. Control* **2016**, *63*, 1704–1721. [[CrossRef](#)] [[PubMed](#)]
15. Sengupta, P.P.; Pedrizzetti, G.; Kilner, P.J.; Kheradvar, A.; Ebbers, T.; Tonti, G.; Fraser, A.G.; Narula, J. Emerging trends in CV flow visualization. *JACC Cardiovasc. Imaging* **2012**, *5*, 305–316. [[CrossRef](#)] [[PubMed](#)]
16. Goddi, A.; Fanizza, M.; Bortolotto, C.; Raciti, M.V.; Fiorina, I.; He, X.; Du, Y.; Calliada, F. Vector flow imaging techniques: An innovative ultrasonographic technique for the study of blood flow. *J. Clin. Ultrasound* **2017**, *45*, 582–588. [[CrossRef](#)] [[PubMed](#)]
17. Shattuck, D.P.; Weinschenker, M.D.; Smith, S.W.; von Ramm, O.T. Explososcan: A parallel processing technique for high speed ultrasound imaging with linear phased arrays. *J. Acoust. Soc. Am.* **1984**, *75*, 1273–1282. [[CrossRef](#)] [[PubMed](#)]
18. Tanter, M.; Fink, M. Ultrafast imaging in biomedical ultrasound. *IEEE Trans. Ultrason. Ferroelectr. Freq. Control* **2014**, *61*, 102–119. [[CrossRef](#)] [[PubMed](#)]
19. Jensen, J.A.; Holm, O.; Jensen, L.J.; Bendsen, H.; Nikolov, S.I.; Tomov, B.G.; Munk, P.; Hansen, M.; Salomonsen, K.; Hansen, J.; et al. Ultrasound research scanner for real-time synthetic aperture data acquisition. *IEEE Trans. Ultrason. Ferroelectr. Freq. Control* **2005**, *52*, 881–891. [[CrossRef](#)] [[PubMed](#)]
20. Lu, J.Y.; Cheng, J.; Wang, J. High frame rate imaging system for limited diffraction array beam imaging with square-wave aperture weightings. *IEEE Trans. Ultrason. Ferroelectr. Freq. Control* **2006**, *53*, 1796–1811. [[CrossRef](#)] [[PubMed](#)]
21. Tortoli, P.; Bassi, L.; Boni, E.; Dallai, A.; Guidi, F.; Ricci, S. ULA-OP: An advanced open platform for ultrasound research. *IEEE Trans. Ultrason. Ferroelectr. Freq. Control* **2009**, *56*, 2207–2216. [[CrossRef](#)] [[PubMed](#)]
22. Daigle, R.E. Ultrasound Imaging System with Pixel Oriented Processing. U.S. Patent 8,287,456B2, 16 October 2012.
23. Jensen, J.A.; Holten-Lund, H.; Nilsson, R.T.; Hansen, M.; Larsen, U.D.; Domsten, R.P.; Tomov, B.G.; Stuart, M.B.; Nikolov, S.I.; Pihl, M.J.; et al. SARUS: A synthetic aperture real-time ultrasound system. *IEEE Trans. Ultrason. Ferroelectr. Freq. Control* **2013**, *60*, 1838–1852. [[CrossRef](#)] [[PubMed](#)]
24. Boni, E.; Bassi, L.; Dallai, A.; Guidi, F.; Meacci, V.; Ramalli, A.; Ricci, S.; Tortoli, P. ULA-OP 256: A 256-channel open scanner for development and real-time implementation of new ultrasound methods. *IEEE Trans. Ultrason. Ferroelectr. Freq. Control* **2016**, *63*, 1488–1495. [[CrossRef](#)] [[PubMed](#)]
25. Powers, J.; Kremkau, F. Medical ultrasound systems. *Interface Focus* **2011**, *1*, 477–489. [[CrossRef](#)] [[PubMed](#)]
26. Boni, E.; Bassi, L.; Dallai, A.; Meacci, V.; Ramalli, A.; Scaringella, M.; Guidi, F.; Ricci, S.; Tortoli, P. Architecture of an ultrasound system for continuous real-time high frame rate imaging. *IEEE Trans. Ultrason. Ferroelectr. Freq. Control* **2017**, *64*, 1276–1284. [[CrossRef](#)] [[PubMed](#)]
27. So, H.; Chen, J.; Yiu, B.; Yu, A. Medical ultrasound imaging: To GPU or not to GPU? *IEEE Micro* **2011**, *31*, 54–65. [[CrossRef](#)]
28. Yiu, B.Y.S.; Tsang, I.K.H.; Yu, A.C.H. GPU-based beamformer: Fast realization of plane wave compounding and synthetic aperture imaging. *IEEE Trans. Ultrason. Ferroelectr. Freq. Control* **2011**, *58*, 1698–1705. [[CrossRef](#)] [[PubMed](#)]
29. Martin-Arguedas, C.J.; Romero-Laorden, D.; Martinez-Graullera, O.; Perez-Lopez, M.; Gomez-Ullate, L. An ultrasonic imaging system based on a new SAFT approach and a GPU beamformer. *IEEE Trans. Ultrason. Ferroelectr. Freq. Control* **2012**, *59*, 1402–1412. [[CrossRef](#)] [[PubMed](#)]
30. Yiu, B.Y.S.; Yu, A.C.H. GPU-based minimum variance beamformer for synthetic aperture imaging of the eye. *Ultrasound Med. Biol.* **2015**, *41*, 871–883. [[CrossRef](#)] [[PubMed](#)]
31. Chang, L.W.; Hsu, K.H.; Li, P.C. Graphics processing unit-based high-frame-rate color doppler ultrasound processing. *IEEE Trans. Ultrason. Ferroelectr. Freq. Control* **2009**, *56*, 1856–1860. [[CrossRef](#)] [[PubMed](#)]
32. Rosenzweig, S.; Palmeri, M.; Nightingale, K. GPU-based real-time small displacement estimation with ultrasound. *IEEE Trans. Ultrason. Ferroelectr. Freq. Control* **2011**, *58*, 399–405. [[CrossRef](#)] [[PubMed](#)]
33. Chee, A.J.Y.; Yiu, B.Y.S.; Yu, A.C.H. A GPU-parallelized Eigen-based clutter filter framework for ultrasound color flow imaging. *IEEE Trans. Ultrason. Ferroelectr. Freq. Control* **2017**, *64*, 150–163. [[CrossRef](#)] [[PubMed](#)]
34. Broxvall, M.; Emilsson, K.; Thunberg, P. Fast GPU based adaptive filtering of 4D echocardiography. *IEEE Trans. Med. Imaging* **2012**, *31*, 1165–1172. [[CrossRef](#)] [[PubMed](#)]
35. Tanter, M.; Bercoff, J.; Sandrin, L.; Fink, M. Ultrafast compound imaging for 2-D motion vector estimation: Application to transient elastography. *IEEE Trans. Ultrason. Ferroelectr. Freq. Control* **2002**, *49*, 1363–1374. [[CrossRef](#)] [[PubMed](#)]

36. Lewandowski, M.; Walczak, M.; Witek, B.; Kulesza, P.; Sielewicz, K. Modular & scalable ultrasound platform with GPU processing. In Proceedings of the 2012 IEEE International Ultrasonics Symposium (IUS), Dresden, Germany, 7–10 October 2012. [[CrossRef](#)]
37. Cheung, C.; Yu, A.; Salimi, N.; Yiu, B.; Tsang, I.; Kerby, B.; Azar, R.; Dickie, K. Multi-channel pre-beamformed data acquisition system for research on advanced ultrasound imaging methods. *IEEE Trans. Ultrason. Ferroelectr. Freq. Control* **2012**, *59*, 243–253. [[CrossRef](#)] [[PubMed](#)]
38. Bercoff, J. Ultrafast ultrasound imaging. In *Ultrasound Imaging-Medical Applications*; Minin, I.V., Minin, O.V., Eds.; InTech: New York, NY, USA, 2011; pp. 3–24.
39. Hansen, K.L.; Møller-Sørensen, H.; Pedersen, M.M.; Hansen, P.M.; Kjaergaard, J.; Lund, J.T.; Nilsson, J.C.; Jensen, J.A.; Nielsen, M.B. First report on intraoperative vector flow imaging of the heart among patients with healthy and diseased aortic valves. *Ultrasonics* **2015**, *56*, 243–250. [[CrossRef](#)] [[PubMed](#)]
40. Goddi, A.; Bortolotto, C.; Fiorina, I.; Raciti, M.V.; Fanizza, M.; Turpini, E.; Boffelli, G.; Calliada, F. High-frame rate vector flow imaging of the carotid bifurcation. *Insights Imaging* **2017**, *8*, 319–328. [[CrossRef](#)] [[PubMed](#)]
41. Jensen, J.A.; Nikolov, S.I.; Gammelmark, K.L.; Pedersen, M.H. Synthetic aperture ultrasound imaging. *Ultrasonics* **2006**, *44*, e5–e15. [[CrossRef](#)] [[PubMed](#)]
42. Montaldo, G.; Tanter, M.; Bercoff, J.; Bencech, N.; Fink, M. Coherent plane-wave compounding for very high frame rate ultrasonography and transient elastography. *IEEE Trans. Ultrason. Ferroelectr. Freq. Control* **2009**, *56*, 489–506. [[CrossRef](#)] [[PubMed](#)]
43. Nikolov, S.I.; Jensen, J.A. In-vivo synthetic aperture flow imaging in medical ultrasound. *IEEE Trans. Ultrason. Ferroelectr. Freq. Control* **2003**, *50*, 848–856. [[CrossRef](#)] [[PubMed](#)]
44. Yiu, B.Y.S.; Yu, A.C.H. Least-squares multi-angle Doppler estimators for plane-wave vector flow imaging. *IEEE Trans. Ultrason. Ferroelectr. Freq. Control* **2016**, *63*, 1733–1744. [[CrossRef](#)] [[PubMed](#)]
45. Hansen, H.H.G.; Saris, A.E.C.M.; Vaka, N.R.; Nillesen, M.M.; de Korte, C.L. Ultrafast vascular strain compounding using plane wave transmission. *J. Biomech.* **2014**, *47*, 815–823. [[CrossRef](#)] [[PubMed](#)]
46. Kruizinga, P.; Mastik, F.; van den Oord, S.C.H.; Schinkel, A.F.L.; Bosch, J.G.; de Jong, N.; van Soest, G.; van der Steen, A.F.W. High-definition imaging of carotid artery wall dynamics. *Ultrasound Med. Biol.* **2014**, *40*, 2392–2403. [[CrossRef](#)] [[PubMed](#)]
47. Kruizinga, P.; Mastik, F.; Bosch, J.G.; De Jong, N.; Van Der Steen, A.F.W.; Van Soest, G. Measuring submicrometer displacement vectors using high-frame-rate ultrasound imaging. *IEEE Trans. Ultrason. Ferroelectr. Freq. Control* **2015**, *62*, 1733–1744. [[CrossRef](#)] [[PubMed](#)]
48. Li, F.; He, Q.; Huang, C.; Liu, K.; Shao, J.; Luo, J. High frame rate and high line density ultrasound imaging for local pulse wave velocity estimation using motion matching: A feasibility study on vessel phantoms. *Ultrasonics* **2016**, *67*, 41–54. [[CrossRef](#)] [[PubMed](#)]
49. Strachinaru, M.; Bosch, J.G.; van Dalen, B.M.; van Gils, L.; van der Steen, A.F.W.; de Jong, N.; Geleijnse, M.L.; Vos, H.J. Cardiac shear wave elastography using a clinical ultrasound system. *Ultrasound Med. Biol.* **2017**, *43*, 1596–1606. [[CrossRef](#)] [[PubMed](#)]
50. Ishii, T.; Yiu, B.Y.S.; Yu, A.C.H. Vector flow visualization of urinary flow dynamics in a bladder outlet obstruction model. *Ultrasound Med. Biol.* **2017**, *43*, 2601–2610. [[CrossRef](#)] [[PubMed](#)]
51. Cikes, M.; Tong, L.; Sutherland, G.R.; D’hooge, J. Ultrafast cardiac ultrasound imaging: Technical principles, applications, and clinical benefits. *JACC Cardiovasc. Imaging* **2014**, *7*, 812–823. [[CrossRef](#)] [[PubMed](#)]
52. Tong, L.; Ramalli, A.; Tortoli, P.; Fradella, G.; Cacioli, S.; Luo, J.; D’hooge, J. Wide-angle tissue doppler imaging at high frame rate using multi-line transmit beamforming: An experimental validation in vivo. *IEEE Trans. Med. Imaging* **2016**, *35*, 521–528. [[CrossRef](#)] [[PubMed](#)]
53. Faurie, J.; Baudet, M.; Assi, K.C.; Auger, D.; Gilbert, G.; Tournoux, F.; Garcia, D. Intracardiac vortex dynamics by high-frame-rate Doppler vortography—In vivo comparison with vector flow mapping and 4-D flow MRI. *IEEE Trans. Ultrason. Ferroelectr. Freq. Control* **2016**, *64*, 424–432. [[CrossRef](#)] [[PubMed](#)]
54. Van Cauwenberge, J.; Lovstakken, L.; Fadnes, S.; Rodriguez-Morales, A.; Vierendeels, J.; Segers, P.; Swillens, A. Assessing the performance of ultrafast vector flow imaging in the neonatal heart via multiphysics modeling and in vitro experiments. *IEEE Trans. Ultrason. Ferroelectr. Freq. Control* **2016**, *63*, 1772–1785. [[CrossRef](#)] [[PubMed](#)]
55. Tremblay-Darveau, C.; Williams, R.; Milot, L.; Bruce, M.; Burns, P.N. Visualizing the tumor microvasculature with a nonlinear plane-wave Doppler imaging scheme based on amplitude modulation. *IEEE Trans. Med. Imaging* **2016**, *35*, 699–709. [[CrossRef](#)] [[PubMed](#)]

56. Correia, M.; Provost, J.; Tanter, M.; Pernot, M. 4D ultrafast ultrasound flow imaging: In vivo quantification of arterial volumetric flow rate in a single heartbeat. *Phys. Med. Biol.* **2016**, *61*, L48–L61. [[CrossRef](#)] [[PubMed](#)]
57. Hansen, K.; Udesen, J.; Gran, F.; Jensen, J.; Bachmann Nielsen, M. In-vivo examples of flow patterns with the fast vector velocity ultrasound method. *Ultraschall Med.* **2009**, *30*, 471–477. [[CrossRef](#)] [[PubMed](#)]
58. Rossini, L.; Martinez-Legazpi, P.; Vu, V.; Fernández-Friera, L.; Pérez del Villar, C.; Rodríguez-López, S.; Benito, Y.; Borja, M.G.; Pastor-Escuredo, D.; Yotti, R.; et al. A clinical method for mapping and quantifying blood stasis in the left ventricle. *J. Biomech.* **2016**, *49*, 2152–2161. [[CrossRef](#)] [[PubMed](#)]
59. Hansen, K.L.; Møller-Sørensen, H.; Kjaergaard, J.; Jensen, M.B.; Lund, J.T.; Pedersen, M.M.; Lange, T.; Jensen, J.A.; Nielsen, M.B. Analysis of systolic backflow and secondary helical blood flow in the ascending aorta using vector flow imaging. *Ultrasound Med. Biol.* **2016**, *42*, 899–908. [[CrossRef](#)] [[PubMed](#)]
60. Hansen, K.L.; Udesen, J.; Oddershede, N.; Henze, L.; Thomsen, C.; Jensen, J.A.; Nielsen, M.B. In vivo comparison of three ultrasound vector velocity techniques to MR phase contrast angiography. *Ultrasonics* **2009**, *49*, 659–667. [[CrossRef](#)] [[PubMed](#)]
61. Swillens, A.; Segers, P.; Torp, H.; Løvstakken, L. Two-dimensional blood velocity estimation with ultrasound: Speckle tracking versus crossed-beam vector doppler based on flow simulations in a carotid bifurcation model. *IEEE Trans. Ultrason. Ferroelectr. Freq. Control* **2010**, *57*, 327–339. [[CrossRef](#)] [[PubMed](#)]
62. Chee, A.J.Y.; Ho, C.K.; Yiu, B.Y.S.; Yu, A.C.H. Walled Carotid Bifurcation Phantoms for Imaging Investigations of Vessel Wall Motion and Blood Flow Dynamics. *IEEE Trans. Ultrason. Ferroelectr. Freq. Control* **2016**, *63*, 1852–1864. [[CrossRef](#)] [[PubMed](#)]
63. Hoskins, P.R. Simulation and Validation of Arterial Ultrasound Imaging and Blood Flow. *Ultrasound Med. Biol.* **2008**, *34*, 693–717. [[CrossRef](#)] [[PubMed](#)]
64. Greyling, A.; van Mil, A.C.C.M.; Zock, P.L.; Green, D.J.; Ghiadoni, L.; Thijssen, D.H. Adherence to guidelines strongly improves reproducibility of brachial artery flow-mediated dilation. *Atherosclerosis* **2016**, *248*, 196–202. [[CrossRef](#)] [[PubMed](#)]
65. Failla, M.; Grappiolo, A.; Emanuelli, G.; Vitale, G.; Fraschini, N.; Bigoni, M.; Grieco, N.; Denti, M.; Giannattasio, C.; Mancia, G. Sympathetic tone restrains arterial distensibility of healthy and atherosclerotic subjects. *J. Hypertens.* **1999**, *17*, 1117–1123. [[CrossRef](#)] [[PubMed](#)]
66. Swierblewska, E.; Hering, D.; Kara, T.; Kunicka, K.; Kruszewski, P.; Bieniaszewski, L.; Boutouyrie, P.; Somers, V.K.; Narkiewicz, K. An independent relationship between muscle sympathetic nerve activity and pulse wave velocity in normal humans. *J. Hypertens.* **2010**, *28*, 979–984. [[CrossRef](#)] [[PubMed](#)]
67. Van Bortel, L.M.; Laurent, S.; Boutouyrie, P.; Chowienczyk, P.; Cruickshank, J.K.; De Backer, T.; Filipovsky, J.; Huybrechts, S.; Mattace-Raso, F.U.S.; Protogerou, A.D.; et al. Expert consensus document on the measurement of aortic stiffness in daily practice using carotid-femoral pulse wave velocity. *J. Hypertens.* **2012**, *30*, 445–448. [[CrossRef](#)] [[PubMed](#)]
68. Thijssen, D.H.J.; Black, M.A.; Pyke, K.E.; Padilla, J.; Atkinson, G.; Harris, R.A.; Parker, B.; Widlansky, M.E.; Tschakovsky, M.E.; Green, D.J. Assessment of flow-mediated dilation in humans: A methodological and physiological guideline. *Am. J. Physiol. Heart Circ. Physiol.* **2011**, *300*, H2–H12. [[CrossRef](#)] [[PubMed](#)]
69. Papamichael, C.M.; Aznaouridis, K.A.; Karatzis, E.N.; Karatzi, K.N.; Stamatelopoulos, K.S.; Vamvakou, G.; Lekakis, J.P.; Mavrikakis, M.E. Effect of coffee on endothelial function in healthy subjects: The role of caffeine. *Clin. Sci.* **2005**, *109*, 55–60. [[CrossRef](#)] [[PubMed](#)]
70. Hijmering, M.L.; de Lange, D.W.; Lorscheid, A.; Kraaijenhagen, R.J.; van de Wiel, A. Binge drinking causes endothelial dysfunction, which is not prevented by wine polyphenols: A small trial in healthy volunteers. *Neth. J. Med.* **2007**, *65*, 29–35. [[PubMed](#)]
71. Dawson, E.A.; Whyte, G.P.; Black, M.A.; Jones, H.; Hopkins, N.; Oxborough, D.; Gaze, D.; Shave, R.E.; Wilson, M.; George, K.P.; et al. Changes in vascular and cardiac function after prolonged strenuous exercise in humans. *J. Appl. Physiol.* **2008**, *105*, 1562–1568. [[CrossRef](#)] [[PubMed](#)]
72. Tinken, T.M.; Thijssen, D.H.J.; Hopkins, N.; Black, M.A.; Dawson, E.A.; Minson, C.T.; Newcomer, S.C.; Laughlin, M.H.; Cable, N.T.; Green, D.J. Impact of shear rate modulation on vascular function in humans. *Hypertension* **2009**, *54*, 278–285. [[CrossRef](#)] [[PubMed](#)]
73. Doonan, R.J.; Hausvater, A.; Scallan, C.; Mikhailidis, D.P.; Pilote, L.; Daskalopoulou, S.S. The effect of smoking on arterial stiffness. *Hypertens. Res.* **2010**, *33*, 398–410. [[CrossRef](#)] [[PubMed](#)]
74. Ahuja, K.D.; Robertson, I.K.; Ball, M.J. Acute effects of food on postprandial blood pressure and measures of arterial stiffness in healthy humans. *Am. J. Clin. Nutr.* **2009**, *90*, 298–303. [[CrossRef](#)] [[PubMed](#)]

75. Novak, V.; Novak, P. Influence of respiration on heart rate and blood pressure fluctuations. *J. Appl. Physiol.* **1993**, *74*, 617–626. [[CrossRef](#)] [[PubMed](#)]
76. Gingham, C.; Beladan, C.C.; Iancu, M.; Calin, A.; Popescu, B.A. Respiratory maneuvers in echocardiography: A review of clinical applications. *Cardiovasc. Ultrasound* **2009**, *7*, 42. [[CrossRef](#)] [[PubMed](#)]
77. Cinthio, M.; Ahlgren, Å.R.; Bergkvist, J.; Jansson, T.; Persson, H.W.; Lindström, K. Longitudinal movements and resulting shear strain of the arterial wall. *Am. J. Physiol. Heart Circ. Physiol.* **2006**, *291*, H394–H402. [[CrossRef](#)] [[PubMed](#)]
78. Schulz, K.F.; Altman, D.G.; Moher, D.; Jüni, P.; Altman, D.; Egger, M.; Chan, A.; Altman, D.; Glasziou, P.; Meats, E.; et al. CONSORT 2010 Statement: Updated guidelines for reporting parallel group randomised trials. *BMC Med.* **2010**, *8*, 18. [[CrossRef](#)] [[PubMed](#)]
79. Hines, E.A.; Brown, G.E. The cold pressor test for measuring the reactivity of the blood pressure: Data concerning 571 normal and hypertensive subjects. *Am. Heart J.* **1936**, *11*, 1–9. [[CrossRef](#)]
80. Saab, P.G.; Llabre, M.M.; Hurwitz, B.E.; Schneiderman, N.; Wohlgenuth, W.; Durel, L.A.; Massie, C.; Nagel, J. The cold pressor test: Vascular and myocardial response patterns and their stability. *Psychophysiology* **1993**, *30*, 366–373. [[CrossRef](#)] [[PubMed](#)]
81. Kline, K.A.; Saab, P.G.; Llabre, M.M.; Spitzer, S.B.; Evans, J.D.; McDonald, P.A.G.; Schneiderman, N. Hemodynamic response patterns: Responder type differences in reactivity and recovery. *Psychophysiology* **2002**, *39*, 739–746. [[CrossRef](#)] [[PubMed](#)]
82. Flück, D.; Ainslie, P.N.; Bain, A.R.; Wildfong, K.W.; Morris, L.E.; Fisher, J.P. Extra- and intracranial blood flow regulation during the cold pressor test: Influence of age. *J. Appl. Physiol.* **2017**, *123*, 1071–1080. [[CrossRef](#)] [[PubMed](#)]
83. Au, J.S.; Bochnak, P.A.; Valentino, S.E.; Cheng, J.L.; Stöhr, E.J. Cardiac and haemodynamic influence on carotid artery longitudinal wall motion. *Exp. Physiol.* **2018**, *103*, 141–152. [[CrossRef](#)] [[PubMed](#)]
84. Lo, A.; Oehley, M.; Bartlett, A.; Adams, D.; Blyth, P.; Al-Ali, S. Anatomical variations of the common carotid artery bifurcation. *AZN J. Surg.* **2006**, *76*, 970–972. [[CrossRef](#)] [[PubMed](#)]
85. Schulz, U.G.R.; Rothwell, P.M. Major variation in carotid bifurcation anatomy: A possible risk factor for plaque development? *Stroke* **2001**, *32*, 2522–2529. [[CrossRef](#)] [[PubMed](#)]
86. Hertzog, M.A. Considerations in determining sample size for pilot studies. *Res. Nurs. Health* **2008**, *31*, 180–191. [[CrossRef](#)] [[PubMed](#)]
87. Pepe, M.S. Receiver operating characteristic methodology. *J. Am. Stat. Assoc.* **2000**, *95*, 308–311. [[CrossRef](#)]



© 2018 by the authors. Licensee MDPI, Basel, Switzerland. This article is an open access article distributed under the terms and conditions of the Creative Commons Attribution (CC BY) license (<http://creativecommons.org/licenses/by/4.0/>).